Figure 5.15 Foot image with various kernels applied: a. Original image; b. Smoothing filter from Fig. 5.14a; c. Edge enhancement filter from Fig. 5.14b; d. Edge detection filter from Fig. 5.14c

Spatial enhancement in the frequency domain is achieved by computing the Fourier transform of the image, multiplying the result by a filter transfer function and taking the inverse Fourier transform of this result to create the new enhanced image. The formula for the two-dimensional discrete Fourier transform can be seen in Equation 5.3.

$$F(u,v) = \frac{1}{MN}\sum_{x=0}^{M-1}\sum_{y=0}^{N-1} \mathrm{I}(x,y)e^{-i2\pi(ux/M+vy/N)} \qquad \ldots\ldots\ldots 5.3$$

for u = 0,1,2,….,M-1 and v = 0,1,2,….,N-1.

where: F (u,v) is the Fourier transform of the image I (x,y);

M is the number of columns in I (x,y);

N is the number of rows in I (x,y).

The general form of spatial enhancement in the frequency domain is shown in Equation 5.4 (Gonzalez & Woods, 1992).

$$G\,(\mathrm{u},\mathrm{v}) = H\,(\mathrm{u},\mathrm{v}).F\,(\mathrm{u},\mathrm{v}) \qquad \ldots\ldots\ldots 5.4$$

where: F (u,v) is the Fourier transform of I (x,y);

H (u,v)is the filter transform function;

G (u,v) is the result prior to performing inverse Fourier transformation to produce O (x,y)

The values of the two dimensional Fourier transform, F(u,v), of an image can be considered as being a Cartesian plot of the Fourier values. An example of the graphical plot of the Fourier transform of the foot image in Figure 5.15a. is shown in Figure 5.16. The values plotted in Figure 5.16 are the magnitudes of the complex Fourier values, plotted on a logarithmic scale and displayed as a grey-scale image. The numbers of rows and columns of plot of F(u,v) are the same as the numbers of rows and columns of I(x,y). The plot of F(u,v) has its origin at (u = 0, v = 0) which is at the centre of the Fourier space. Low frequency values are located near the centre of the Fourier space and higher frequency values are located towards the edges of the Fourier space (Castleman, 1996; Gonzalez & Woods, 1992; Russ, 1994).

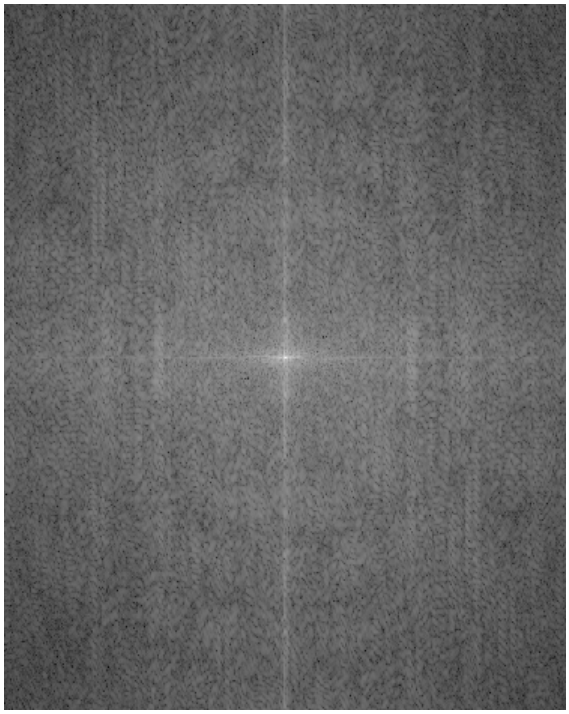

Figure 5.16 Fourier transform of foot image from Figure 5.15a

The type of enhancement of the image that results from frequency domain enhancement depends upon the design of $H(u,v)$. Examples of filters used for low pass filtering are box filters, triangular filters, Gaussian filters and Butterworth low pass filters. Examples of filters used for high pass filtering are Laplacian filters, differential-of-Gaussian filters and Butterworth high pass filters (Castleman, 1996; Gonzalez & Woods, 1992; Russ, 1994). An example of an ideal low pass filter is shown in Figure 5.17 and an example of an ideal high pass filter is shown in Figure 5.18 (Gonzalez & Woods, 1992). A type of filtering that is difficult to achieve in the spatial domain is band pass filtering. Such filters enhance or act upon a specific range of frequencies in $F(u,v)$. No enhancement occurs above and below this range of frequencies.

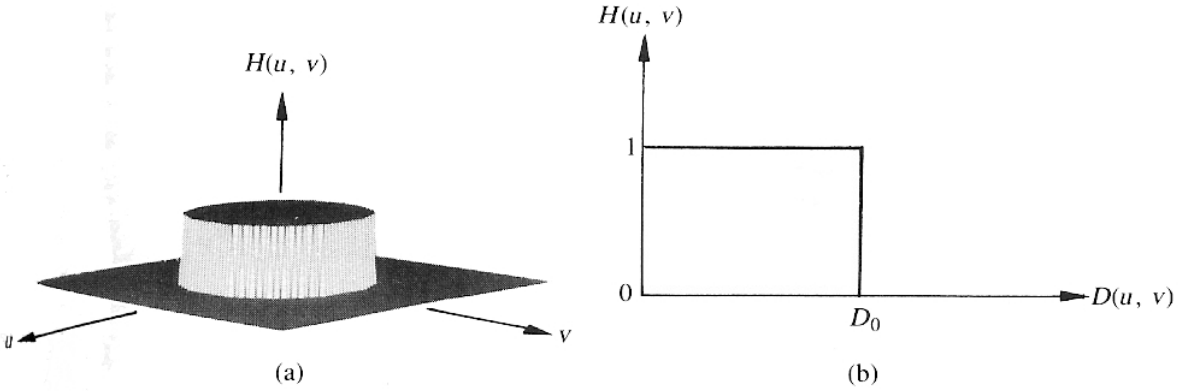

Figure 5.17 Ideal low pass filter design for frequency domain image enhancement (Gonzalez & Woods, 1992, p.203)

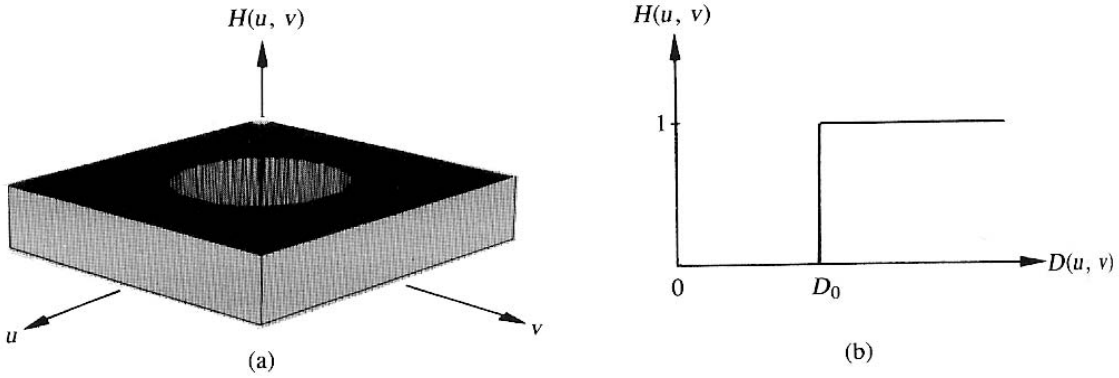

Figure 5.18 Ideal high pass filter design for frequency domain image enhancement (Gonzalez & Woods, 1992, p.212)

5.6 Unsharp Masks

A typical spatial enhancement technique used in DR is unsharp masking (Giger & MacMahon, 1996; Prokop & Schaefer-Prokop, 1997; Prokop *et al*, 1993; Van Metter & Foos, 1999a, 1999b; Vuylsteke & Schoeters, 1994, 1999). The unsharp masked method is based on an analogue process used with photographic film to slightly enhance edges in the image. It involves blurring or smoothing of the original image and subtracting this image from the original, leaving only the edges of features in the image. A weighting factor is applied to the new edge image which then is added to the original image (Baxes, 1994; Gonzalez & Woods, 1992; Jain, 1989; Russ, 1994). A general form of the unsharp masking process can be seen in Equation 5.5.

$$O(x, y) = I(x, y) + wf \cdot (I(x,y) - S(x,y)) \qquad \ldots\ldots\ldots 5.5$$

where: O (x,y) is the new or output image;
I (x,y) is the original image;
S (x,y) is the smoothed or blurred image of I (x, y);
wf is the weighting factor.

The amount of smoothing of the features will determine the degree of edges that remain following subtraction of S(x,y) from I(x,y). This and the weighting factor control the degree of edge enhancement of the image. This is the preferred method to enhance edges or high frequency features of DR images.

Unsharp mask results can also be achieved by using local neighbourhood operations with kernels of appropriate size and value. Unsharp kernels have the same characteristics as edge enhancement kernels. The central value of the unsharp mask kernel is less than the central value of edge enhancement kernels discussed previously. A comparison of 3x3 kernels is shown in Figure 5.19. Figure 5.19a kernel is a typical standard edge enhancement kernel and Figure 5.19b & c. are unsharp mask kernels. The values in 5.19b & c. were obtained by performing the operation in Equation 5.3 on an impulse function with a value of 1 and with a *wf* of 1

and 1.5 respectively. A comparison of DR foot images with standard edge enhancement and unsharp mask filters is provided in Figures 5.20a, b & c.

-1	-1	-1
-1	9	-1
-1	-1	-1

a.

-0.111	-0.111	-0.111
-0.111	1.889	-0.111
-0.111	-0.111	-0.111

b.

-0.1667	-0.1667	-0.1667
-0.1667	2.33335	-0.1667
-0.1667	-0.1667	-0.1667

c

Figure 5.19 Comparison of standard edge enhancement kernel and unsharp mask kernels:

a. Standard edge enhancement kernel;
b. Unsharp mask kernel, *wf* = 1;
c. Unsharp mask kernel, *wf* = 1.5.

The image in Figure 5.20b has edge enhancement that is too strong for adequate visualisation of the anatomy and pathology within the image. This is not fully apparent at the displayed size of this image. This image also exhibits an increase in noise compared to the original image, Figure 5.20a. The unsharp mask process in Figure 5.20c has resulted in less edge enhancement than in the image in Figure 5.20b. There is also less noise in the image compared to the image in Figure 5.20b. Again, the effects of this filter are not fully apparent at the displayed size of this image.

a. b.

c.

Figure 5.20 Comparison of foot image with various kernels applied:

a. Original image; b. Standard edge enhancement filter from Fig. 5.19a;

c. Unsharp mask kernel from Fig. 5.19b.

High degrees of edge enhancement can also introduce artefactual appearances in the image. Over-emphasising the high frequency components in the image can create white and black lines along edges within the image. So-called halo or rebound artefacts become visible. These artefactual appearances are more prominent when there are large contrast differences at the edge, such as when metal protheses are present (Cesar *et al*, 2001; Murphey, 1992; Murphey *et al*, 1997; Vuylsteke & Schoeters, 1999). These aspects were discussed in Chapter 4. Such artefacts are reduced when unsharp mask processes are used compared to when full edge enhancement filters are used.

Unsharp mask filtering used in commercial DR may differ slightly from that discussed above. In such unsharp mask processes, the weighting factor is modified by the local regional pixel values. The general form of unsharp masking used in commercial DR is shown in Equation 5.6 (adapted from Vuylsteke & Schoeters, 1999).

$$O(x, y) = I(x, y) + wf.\beta(a, b).\left(I(x,y) - S(x,y)\right) \quad \ldots\ldots\ldots 5.6$$

where: O (x,y) is the new or output image;
I (x,y) is the original image;
S (x,y) is the smoothed or blurred image of I (x, y);
wf is the weighting factor;
β (a,b) is a function that adapts the degree of enhancement by local regional density values
(adapted from Vuylsteke & Schoeters, 1999).

Unsharp mask kernel size is also varied in DR imaging. Kernel sizes for unsharp mask filtering in DR were compared with sizes from 5 to 109 pixels by Vuylsteke & Schoeters (1999). The shapes of the frequency responses of four unsharp mask filters at different kernel sizes are shown in Figure 5.21 (Vuylsteke & Schoeters, 1999). Kernel sizes of 5, 13, 39 and 109 are shown. Unsharp masks used with small kernel sizes will enhance high frequency or small objects. If this is the desired response within the new or displayed image, the kernel size should be slightly larger than the object or edge that it has been chosen to enhance (Vuylsteke & Schoeters, 1999).

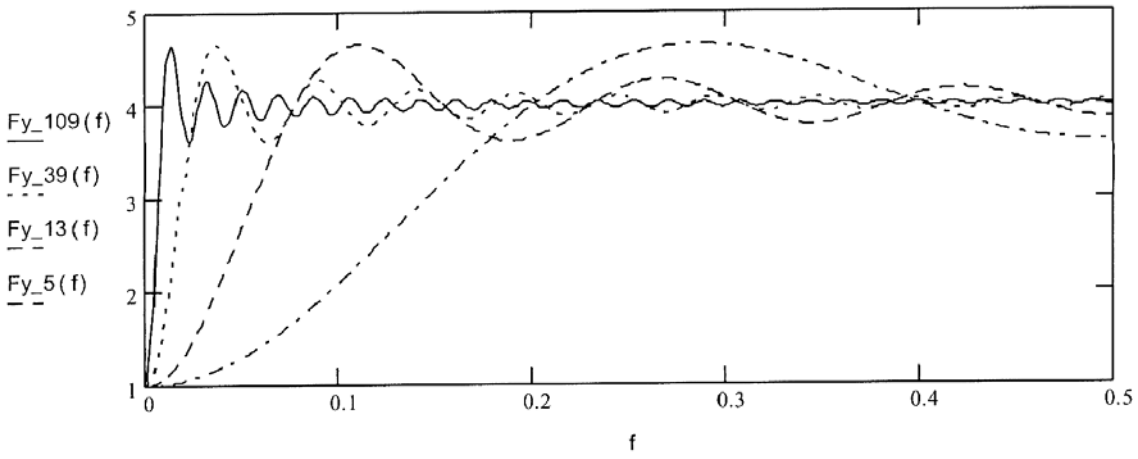

Figure 5.21 Unsharp mask filters with kernel sizes of 5, 13, 39 and 109 (Vuylsteke & Schoeters, 1999, p.559)

Difficulty in selecting the appropriate size kernel of unsharp masks for use in DR imaging has been reported by Prokop *et al* (1993). In their discussion, kernel sizes of small (1.4 mm), medium (5mm), large (25mm) and ultra-large (70mm) were used. These sizes were not given in pixel numbers. Various sized lung nodules were enhanced to greater or lesser extent with the various size filters. Müller *et al* (1996a) also evaluated the appearance of lung nodules using various size unsharp mask kernels. Kernel sizes of 2.83mm, 5.66mm, 11.31mm and 19.8mm were used and compared to F/S images. Large kernel size filtering provided better detectablity of lung nodules than small kernel size filtering.

The image quality of DR images using various size unsharp mask kernels was evaluated by Müller *et al* (1996a). The focus of their study was interstitial lung disease and how it was best displayed using various unsharp mask kernel sizes. Their conclusion was that small unsharp mask kernel sizes were of little value in examining interstitial lung disease, whereas medium sized kernels improved diagnostic performance. Variations of unsharp mark filters have been used with digital x-ray fluoroscopy (Jabri & Wilson, 2002). In that study, Gaussian shaped filters were used to smooth the image. The kernel sizes were 7x7, 19x19 and 39x39 pixels. The purpose of the project was to evaluate the detectability of guide-wires

under fluoroscopic control. The use of unsharp mask filters improved detectability of the guide-wires compared to standard imaging. The small and medium sized kernels were shown to have significantly better performance than the large kernel in detectability of the guide-wires. Noise was also noted as a problem when using such unsharp masks. Noise was greatest when the kernel size used was 7x7. The so-called over-shoot artefacts or halo artefacts discussed previously were also noted when the 7x7 kernel size was used.

Miettunen & Korhola (1991) measured the noise in DR images as a result of applying unsharp masks of various kernel sizes. They concluded that signal-to-noise ratio (SNR) was reduced by more than 40% when small kernel sizes were used. As the kernel size increased, SNR improved. At no time did the SNR reach or exceed the SNR of the original images.

5.7 Dynamic Range Control

The unsharp mask process may also be used to assist in overcoming the problems previously described of large dynamic range in DR images and the difficulty of adequately viewing this range of pixel values. When large to very large kernel sizes are selected, the middle and low frequencies respectively within the image are enhanced (Vuylsteke & Schoeters, 1999). The relative contributions of low frequency components in the image are reduced when very large filter sizes are used. The assumption is that these low frequency components do not carry significant information and, as such, can be repressed. Unsharp mask kernel sizes typically larger than 255 pixels are required for this purpose. This reduces the dynamic range of low frequency areas or objects in the image (Vuylsteke & Schoeters, 1999).

Kodak uses this method with its computed radiography systems. Kodak's process is commercially known as "enhanced visualization processing" (EVP). Van Metter & Foos (1999a) report that EVP is a non-linear unsharp mask process that increases the latitude of the DR image while preserving contrast. It is achieved by reducing the contrast of the low frequency components of the image. The $\beta(a,b)$ from Equation 5.6 is non-linear. High frequency components are preserved to maintain image detail.

EVP uses three parameters to adjust the filter shape. Kernel size adjusts the frequency range, gain controls the latitude, and density controls the values of the low frequency areas (Van Metter & Foos, 1999a).

Prokop *et al* (1993) reported that ultra-large (70mm) unsharp kernel sizes decrease the optical density differences between areas of large contrast difference in the chest. The lungs and the mediastinum were "equalised" when ultra-large unsharp mask kernel sizes were used. This was described as being a form of dynamic range compression. Prokop *et al* also noted that using unsharp mask methods increased the noise in the image.

A further disadvantage of using large kernel unsharp mask filters for dynamic range control was discussed by Prokop & Schaefer-Prokop (1997). Dynamic range compression can only be performed to a certain level. After this level, edge artefacts, similar to the over-shoot artefacts or the halo artefacts discussed previously, appear on the image. According to Prokop & Schaefer-Prokop, the dynamic range compression that results from the use of such kernel sizes for areas such as the thoracolumbar junction may not suffice for adequate viewing. The desired dynamic range compression effect will not be visualised.

An image of both feet, obtained for use in the RCM survey (see Chapter 8 for details), was modified using unmask sharp filter sizes of 21x21, 51x51 and 109x109. The images were modified using the software program Matlab® (MathWorks Inc., Natick, USA). Figure 5.22a, b, c & d allows comparison of these filtered images with the original image. Magnified subsections of these images can be seen in Figure 5.23a, b, c & d.